MAGNETIC RESONANCE

Jaco J. M. Zwanenburg
Jeroen Hendrikse
Fredy Visser
Taro Takahara
Peter R. Luijten

Fluid attenuated inversion recovery (FLAIR) MRI at 7.0 Tesla: comparison with 1.5 and 3.0 Tesla

J. J. M. Zwanenburg · P. R. Luijten
Image Sciences Institute,
University Medical Center Utrecht,
Utrecht, The Netherlands

J. J. M. Zwanenburg (✉) ·
J. Hendrikse · T. Takahara ·
P. R. Luijten
Department of Radiology,
University Medical Center Utrecht,
HP E 01.132,
P.O. Box 85500, 3508 GA
Utrecht, The Netherlands
e-mail: J.J.M.
Zwanenburg@umcutrecht.nl
Tel.: +31-88-7551394
Fax: +31-30-2513399

F. Visser
Philips Healthcare,
Best, The Netherlands

Abstract *Purpose:* To assess fluid-attenuated inversion recovery (FLAIR) magnetic resonance imaging (MRI) at three field strengths, regarding signal-to-noise ratio (SNR), contrast and signal homogeneity, in order to determine the potential gain and current challenges of FLAIR at ultra-high field strength (7 T). *Methods:* FLAIR images of five healthy volunteers (age 24±4 years, 4 male) were acquired at 1.5 T, 3 T and 7 T. Image homogeneity and visibility of normal brain structures were evaluated. SNR of grey matter (GM), white matter (WM) and cerebrospinal fluid (CSF) were measured in regions not affected by transmit field heterogeneity. *Results:* The SNR (mean ± SD) at 7 T (GM 168±15, WM 125± 11) increased slightly more than proportionally, compared with at 1.5 T (GM 30±3, WM 22±2) and 3 T (GM 62±7, WM 44±4). Relative contrast between GM and WM at 7 T (1.35±0.07) was slightly less than at 3 T (1.42±0.14) or 1.5 T (1.37±0.07). Several major fibre bundles became visible at 7 T. One incidentally observed white matter lesion was well visible at all field strengths. *Conclusion:* Image homogeneity remains challenging and should be improved by future technical developments. FLAIR imaging at 7 T yields a high SNR, with better contrast for WM substructures and the iron-bearing basal ganglia, and has potential for good conspicuity of WM lesions.

Keywords T_2-weighted FLAIR · Magnetic resonance imaging · High field strength · Image contrast · Brain

Introduction

T_2-weighted fluid attenuated inversion recovery (FLAIR) imaging is one of the cornerstones of MR neuroimaging protocols. With the nulling of the cerebrospinal fluid (CSF), FLAIR imaging results in an excellent contrast between lesions in the white matter or grey matter and the surrounding brain tissue [1]. For instance, FLAIR imaging is regarded as one of the most sensitive imaging techniques for the detection of white matter lesions, either age related or in patients with multiple sclerosis [2, 3]. FLAIR imaging is nowadays a robust sequence at 1.5 T and 3 T, the clinically most commonly used field strengths [4]. Recently, ultra-high field strength magnets of 7 T have become more widely available. Studies showed that spectroscopy [5], gradient echo imaging [6] and MR angiography sequences [7, 8] benefit most from the increased signal-to-noise (SNR) at 7 T. The combination of a higher SNR and a shorter T_2* is beneficial for BOLD fMRI [9, 10] and susceptibility-weighted imaging [6]. With the wider availability of 7-T magnets interest has increased in the clinical application of ultra-high field MRI, and recently 7-T imaging results of a multiple sclerosis patient were presented, including a FLAIR image [11]. Thus far, however, no studies have compared the current quality of FLAIR imaging at 7 T with FLAIR at the commonly used field strengths 1.5 T and 3 T. For clinical neuroimaging at 7 T, it is crucial to have a FLAIR imaging protocol with comparable quality to those of lower field

strengths. Such a protocol enables an adequate evaluation of abnormalities and a better interpretation of the results from the above-mentioned MR sequences that benefit from an ultra-high field strength.

FLAIR imaging at 7 T is challenging, mainly because of practical issues related to the homogeneity of the magnetic field and limitations in the specific absorption rate (SAR). Image heterogeneity is caused by variations in homogeneity of both the receive field and the transmit field (B_1^+). Variations in the transmit field at 7 T results in spatial variation in excitation and refocusing flip angles, which leads to variable contrast and signal within the acquired images. Inadequate nulling of the CSF may be prevented by the use of an adiabatic inversion pulse, which can achieve full inversion in the presence of substantial inhomogeneities in the main magnetic field and the transmit field [12]. However, adiabatic inversion pulses have a much higher SAR than ordinary pulses. The SAR of an adiabatic pulse can easily be five times higher than the SAR of a plain amplitude modulated pulse.

A more fundamental problem may arise from the field strength dependency of the T_1 relaxation times. Because of the prolonged T_1 relaxation times of grey and white matter (GM and WM), with a relatively constant T_1 of cerebrospinal fluid (CSF) [13], the contrast in FLAIR may be less at ultra-high field strength, as the T_1 contrast counteracts the T_2 contrast. The field-strength-dependent effect of the competing T_1 contrast can be illustrated with straightforward calculations of the magnetisation in an inversion recovery sequence with infinite repetition time. Assuming a perfect inversion pulse and a perfect 90° excitation pulse after the inversion delay TI, the transverse magnetisation following excitation can be shown to be

$$M_{xy} = M_0\left(1 - 2e^{-TI/T_1}\right)e^{-t/T_2}.$$

In this equation, M_{xy} is the transverse magnetisation, M_0 the longitudinal equilibrium magnetisation, and t the time following excitation. A prolonged T_1 at a given TI implies less relaxation and thus more remaining T_1 contrast. This is illustrated in Fig. 1, where both the relaxation of the magnetisation after inversion and the signal after excitation are shown. The field-strength-dependent T_1 values were taken from Rooney et al. [13]. In order to only illustrate the T_1 effects, a single T_2 for GM (90 ms) and WM (60 ms) for all field strengths was used.

Despite these challenges of FLAIR imaging at 7 T, FLAIR imaging may benefit from the increased SNR at ultra-high field strength, similar to other pulse sequences. The present paper assesses the potential of FLAIR imaging at 7 T by concentrating on the image areas that suffer least from variations in the transmit field. According to our experience, adequate nulling of CSF at 7 T can be obtained in the entire brain by using an adiabatic inversion pulse. The subsequent SAR problem can be alleviated by reducing the number of acquired slices, while an increased
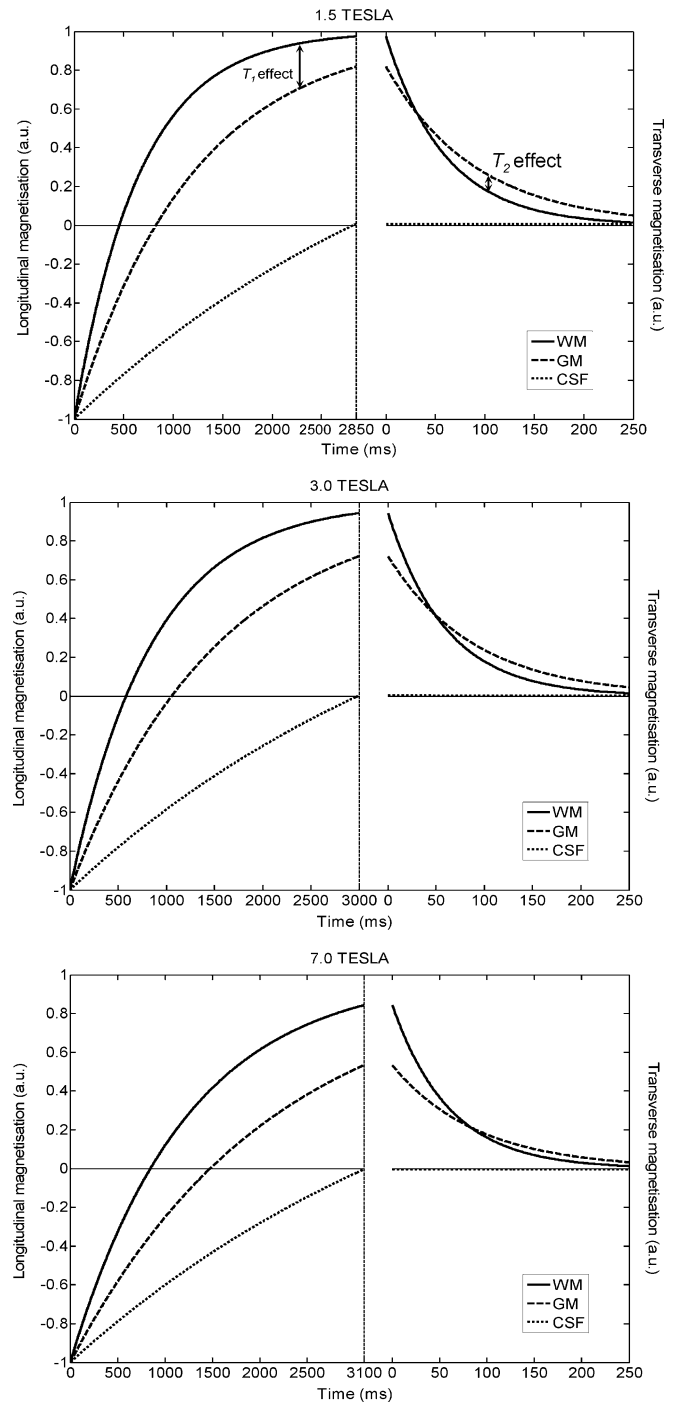

Fig. 1 The longitudinal magnetisation and transverse magnetisation of white matter (*solid curve*), grey matter (*dashed curve*) and CSF (*dotted curve*) during the inversion recovery sequence. The *vertical dashed line* indicates the inversion delay (TI) at which CSF is suppressed and at which a 90° excitation pulse is applied. For clarity, the timescale is made different after excitation. It is clear that the T_2 contrast is counteracted by the incomplete relaxation of GM and WM at TI, as the transverse magnetisation curves cross each other. The competing T_1 effect increases with increasing field strength

slice gap still provides images distributed over the entire brain.

The aim of the present study is to assess fluid-attenuated inversion recovery (FLAIR) magnetic resonance imaging (MRI) at three different field strengths (the most commonly used field strength 1.5 T, high field 3 T and ultra-high field 7 T), regarding signal-to-noise ratio (SNR), contrast and signal homogeneity. This comparison is important in order to understand the potential advantages and current challenges of FLAIR imaging for clinical neuroimaging studies at ultra-high field strength.

Material and methods

Five volunteers (age 24±4 years, 4 male, 1 female) without history of neurological disease were imaged on 1.5-T, 3-T and 7-T MRI (Philips Healthcare), with an 8-channel receive head coil and body transmit coil at 1.5 T and 3 T (max. B_1 13.5 µT), and a 16-channel receive coil with volume T/R coil for transmission (max. B_1 20 µT) at 7 T (Nova Medical, Wilmington, MA, USA). Written informed consent was obtained in accordance with the Institutional Review Board of our hospital.

The parameters of the FLAIR sequence are largely determined by the requirement to null CSF, and the limitations imposed by the SAR constraints, as modelled in the system software. A straightforward comparison of the FLAIR sequences at different field strengths was performed by slightly adjusting the inversion delay (TI) to null CSF on all systems, and by reducing the number of slices at the 7-T system to stay within the SAR limits. Imaging

parameters can be found in Table 1. The inversion pulse for CSF suppression consisted of an adiabatic hyperbolic secant pulse (at all field strengths), which proved to give sufficient inversion for the whole brain at 7 T, despite the inhomogeneity in the transmit field. No SENSE acceleration was applied. The default image homogeneity correction of the MRI system was applied at all field strengths, to correct for image intensity variation induced by the receive coil sensitivity pattern. The noise level for each image was measured by repeating each data acquisition with the same receiver gain for data sampling, without applying any RF pulses or gradients.

A qualitative comparison of the images was performed, regarding heterogeneity in signal intensity and visibility of brain structure at the three field strengths. To assess the SNR, regions of interest (ROIs) were defined at one location in the brain, where signal drop due to transmit field heterogeneity was minimal. The obtained SNR and contrast from these ROIs can be regarded as an indication of the potential of 7-T FLAIR imaging, when the technical limitations of obtaining a homogeneous flip angle are overcome. The used ROIs are illustrated in Fig. 2. The standard deviation of the combined ROIs in the noise image was used as noise metric for the SNR calculation. Relative contrast between GM and WM was defined as SNR_{GM}/SNR_{WM}.

SNR of grey and white matter, and relative contrast between GM and WM were compared among the field strengths using paired t tests. For the relative contrast, single-sided P values are reported, as we expect from theory that the relative contrast will decrease towards higher field strength (yielding a difference in a single

Table 1 Imaging parameters of the T_2-weighted FLAIR sequences at the three different field strengths

	1.5 T	3 T	7 T
FOV (mm^2)	230×183	230×183	230×183
Acquired resolution (mm^2)	0.65×0.88	0.65×0.88	0.65×0.88
Slice thickness (mm)	4	4	4
Slice spacing (mm)	0	0	8
Number of interleaves	3	3	1
Turbo spin-echo factor	26	26	26
Refocusing flip angle (°)	120	120	120
TI (ms)	2,800	2,900	3,100
TR (ms)	14,000	14,000	21,222
TE	125	125	101
Echo spacing	9.3	9.3	7.5
Readout BW (Hz/pixel)	221	221	230
Number of slices	24	24	8
Imaging duration (s)	378	378	191
Estimated SAR (W/kg)	0.3	0.8	1.9

FOV field of view, *TI* inversion delay, *TR* repetition time, *TE* echo time, *BW* bandwidth, *SAR* specific absorption rate
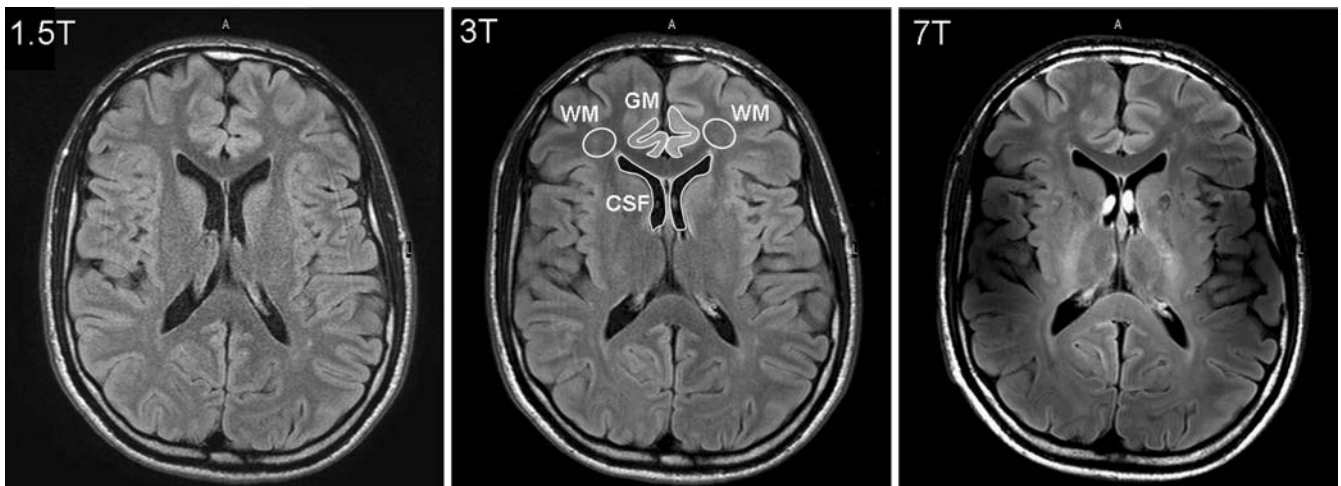
Fig. 2 1.5-T, 3-T and 7-T T_2-weighted FLAIR images with transversal orientation, clearly showing the increase in SNR with increasing field strength. The ROIs used are indicated on the 3-T image, for white matter (*WM*), grey matter (*GM*) and *CSF*. Flow

artefacts (like the *hyperintense dots* in the lateral ventricles on the 7-T image) were excluded from the CSF ROIs, if present. The low image intensity in the temporal lobes at 7 T is a consequence of a low flip angle because of the heterogeneity in the transmit field

direction). A *P* value < 0.05 was considered to be significant.

Results

Figure 3 shows representative FLAIR images of a single subject at all three field strengths. The 7-T images show high SNR and high contrast between different structures in most of the cerebrum. Marked variation in image intensity was observed, with signal loss in the frontal and parietal operculum of the brain, which increased towards the more caudal slices. This variation is caused by the well-known spatial variation in the transmit field. Despite this variation in the transmit field, the signal from CSF was adequately suppressed in all slices.

The SNR values (mean ± SD) at 7 T (GM 168±15, WM 125±11) increased slightly more than proportionally, compared with at 1.5 T (GM 30 ± 3, WM 22±2) and 3 T (GM 62±7, WM 44±4), as illustrated in Fig. 4. The relative contrast at 7 T (1.35±0.07) was slightly less than that at 3 T (1.42±0.14) or 1.5 T (1.37±0.07), but these differences were not significant (*P* = 0.12 and *P*=0.13, respectively). The signal from the CSF was well suppressed at all field strengths. The measured SNR of CSF was 4.3±0.7 for 1.5 T, 5.6±0.9 for 3 T, and 10±3 for 7 T.

Several interesting observations were made. First, at 7 T several white matter structures became much more apparent, which were consistent with the major fibre tracts like the pyramidal tracts and the optic radiation (Fig. 5). Second, there was an increase in contrast in the area of the basal ganglia at high field strength, which is clear from Figs. 3 and 5. This contrast originated mainly from decreased signal in the globus pallidus at 3 T and especially at 7 T. Increased hypointensity was also observed for the

nucleus ruber at 3 T and 7 T. Within the thalamus, subnuclear structures became visible at 7 T (Fig. 5). Third, one of the volunteers had a small incidental white matter lesion, which was plainly visible at all three field strengths. At 7 T, the location of this lesion with respect to the corona radiata could clearly be identified (Fig. 6).

Discussion

The SNR of FLAIR imaging showed a clear, approximately linear, increase from 1.5 T to 3 T and 7 T. A trend was found towards a lower relative grey–white matter contrast with FLAIR imaging at 7 T compared with 1.5 T and 3 T, while the contrast between the basal ganglia increased. Furthermore, white matter structures consistent with major fibre bundles became more apparently visible at 7 T. We showed the possibility of an adequate CSF suppression with FLAIR imaging at 7 T, despite the inhomogeneity of the transmit field. However, severe signal heterogeneities were still present in the region of the temporal lobe and in the cerebellum, which needs to be addressed by future technical developments for adequate FLAIR imaging of the full brain.

As expected we showed a clear SNR increase in FLAIR imaging at 7 T compared with 1.5 T and 3 T. These results are in line with previous studies comparing the signal characteristics of FLAIR at 3 T and 1.5 T, although no formal SNR comparisons were made in these studies [14–16]. Bachman et al. reported SNR and contrast-to-noise values for 1.5 T and 3 T [17]. If one corrects for the difference in voxel size between 1.5 T and 3 T in that study, it appears that there was also an approximately linear increase in SNR with field strength.

Fig. 3 T_2-weighted FLAIR images comparison among 1.5 T, 3 T and 7 T in a single subject. The images have a high SNR and good contrast. Variations in the transmit field causes hypointensity in mainly the temporal lobes at 7 T
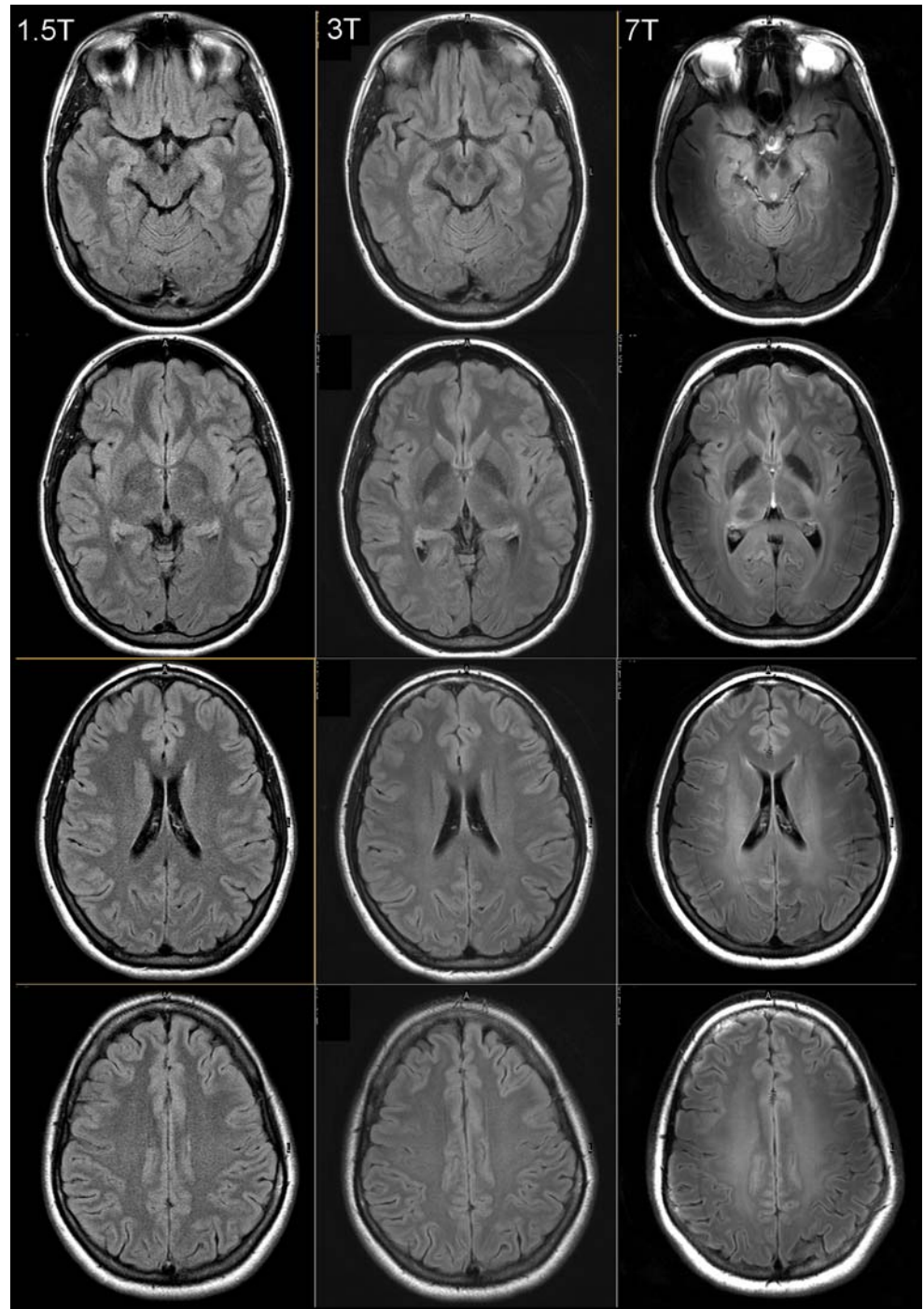
The FLAIR example images suggest that the increased SNR will result in better delineation of white matter lesions, with less noise, from a lower towards a higher field strength. However, a larger 7-T study with patients is needed to investigate the visibility of white matter lesions in different areas in the brain, such as the white matter bundles. Recent studies in MS patients showed that white matter lesions in MS patients are often located in the proximity of veins [11]. For these studies susceptibility-weighted imaging [18] at 7 T might be combined with FLAIR imaging to obtain a high sensitivity for veins and white matter lesions, respectively.

Interestingly, FLAIR imaging at 7 T resulted in a different contrast for several substructures of the brain. Anatomical substructures in the white matter can clearly be distinguished, such as the pyramidal and cortical spinal
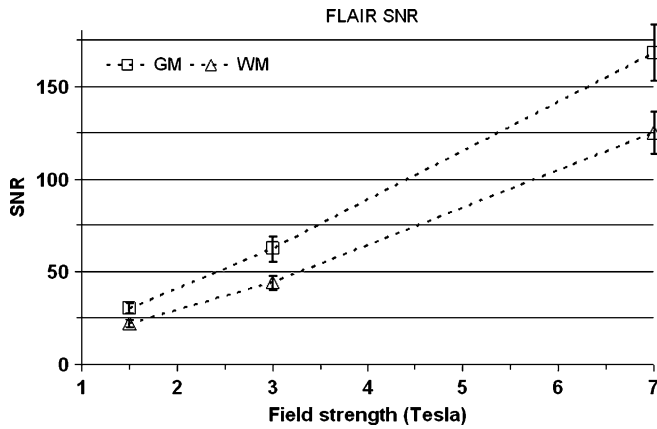
Fig. 4 Signal-to-noise ratios (SNR) of grey matter (*GM*) and white matter (*WM*) increase approximately proportionally with increasing field strength

tracts. Furthermore, we found a clear hypointensity of the globus pallidus and the nucleus ruber at 3 T, but most obviously at 7 T. Also structures in the thalamus became visible at 7 T. The basal ganglia have a relatively high iron content, and hence a relatively short T_2, which may explain the observed hypointensity of these regions.

No significant difference was found in the present study with regard to the relative contrast to noise at different field strengths although a trend was found towards a lower relative contrast at 7 T. As has been illustrated in Fig. 1, the contrast between GM and WM in FLAIR was expected to

be less at ultra-high field strength, as T_1 contrast counteracts the T_2 contrast. Still, this effect was relatively small for the GM and WM ROI analysed in the present study, and not significant within the small number of volunteers. The effect of the competing T_1 contrast may be stronger in other regions of the brain, as the contrast varies throughout the brain as a result of differences in T_1 and T_2 values. Especially for the occipital lobe the grey–white matter contrast is known to be different from that of other regions of the brain. The results may also be different from the straightforward simulations, as the simulations did not take into account the use of multiple refocusing pulses with concomitant magnetisation transfer effects, and the variation in T_2 values across field strengths.

It is worth noting that the visibility of white matter substructures at 7 T is similar to that described by Hajnal et al. [1], in the first publication of the FLAIR technique on a 1.0-T MRI system at a long TE (240 ms). By imaging an infant, Hajnal et al. showed that the T_2-weighted FLAIR signal is sensitive to the degree of myelinisation, as myelinated white matter regions appeared dark and unmyelinated white matter appeared bright. They suggested that the observed contrast within white matter may be explained partly by a small susceptibility difference between myelinated fibres and surrounding tissue. Such a susceptibility difference would induce magnetic field gradients around fibre bundles that are not parallel to the main field, leading to diffusion-induced signal loss in a spin echo. Fibres that are parallel to the main field do not produce susceptibility-
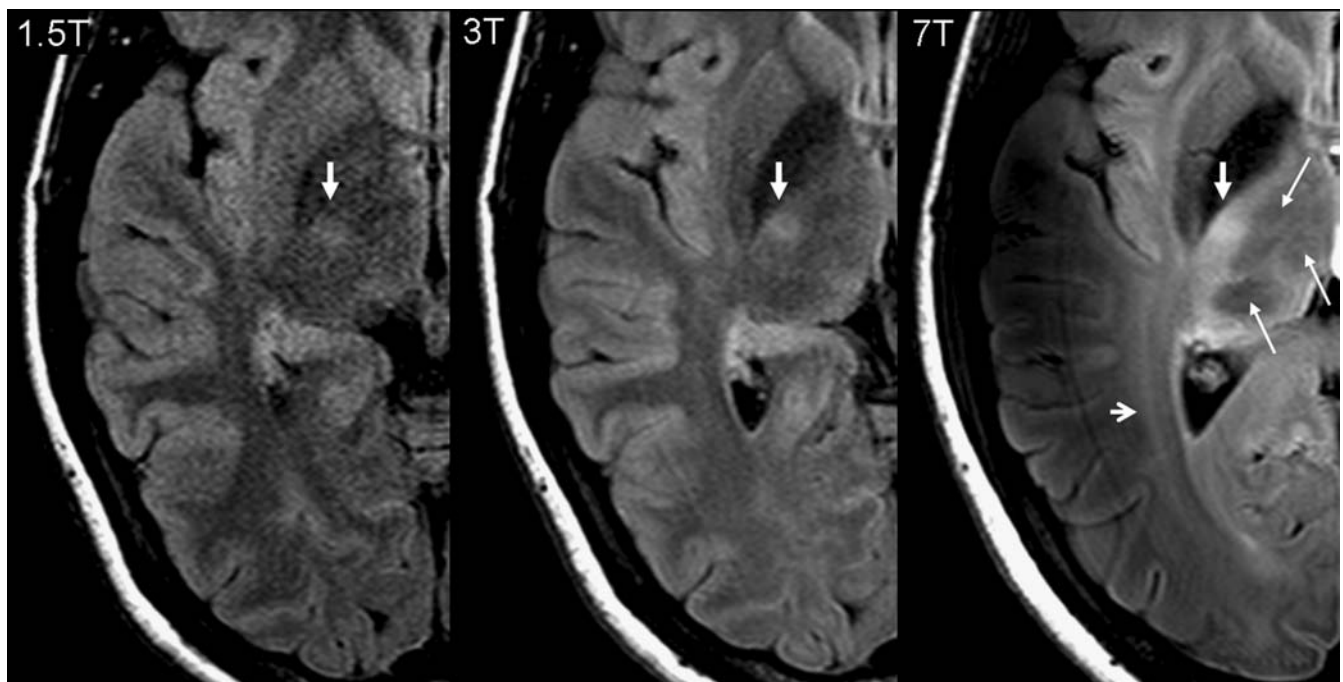

Fig. 5 Zoomed images illustrating the visibility of the pyramidal tract (*closed short arrow*) and optic radiation (*open arrow*) on the 7-T T_2-weighted FLAIR images. Note also the subnuclear structures that are visible in the thalamus at 7 T (*long arrows*)
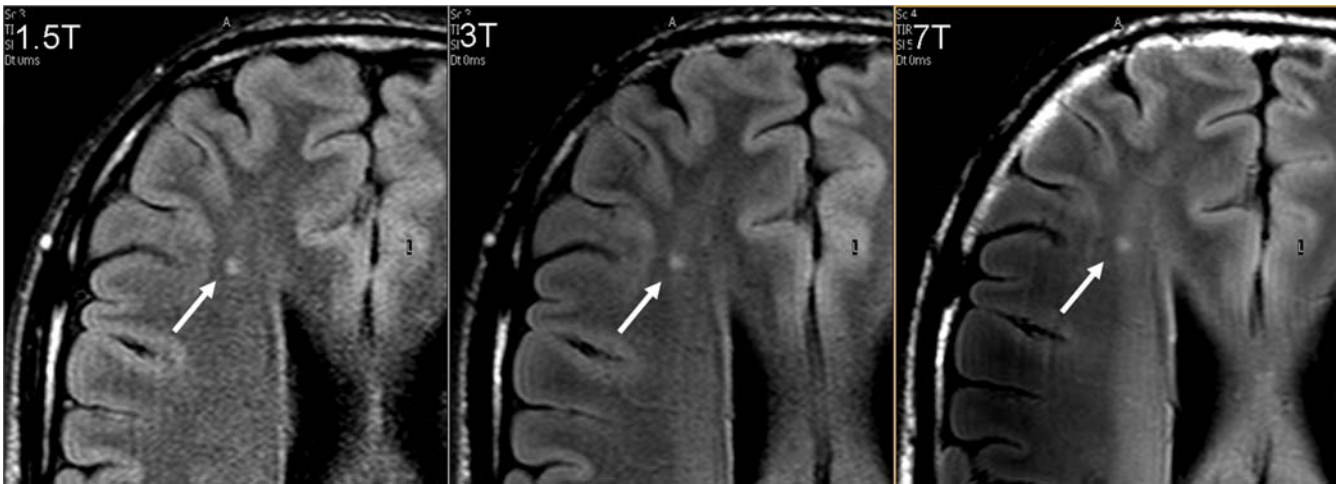
Fig. 6 An incidentally found small white matter lesion was well visible at all three field strengths. The conspicuity of the lesion at 7 T is similar to that at the other field strengths, but the location of the lesion with respect to the main white matter structure is much more distinct. At 7 T, it is easily recognised that the lesion is located on the lateral edge of the corona radiata

induced gradients and will hence have higher signal in a spin echo sequence. The degree of such diffusion-induced signal loss would depend obviously on the strength of the susceptibility-induced gradients and the TE. Because the susceptibility-induced gradients increase with increasing field strength, a small susceptibility difference between myelinated fibres and surrounding tissue would perfectly explain the fact that we obtained a similar contrast as Hajnal, at a much shorter echo time.

Li et al. [6] also observed white matter substructures at 7 T, using T_2*-weighted images, and suggested differences in myelin content, iron concentration and/or fibre direction with respect to the main field as potential contrast mechanisms. It should be noted, however, that the contrast mechanism for T_2-weighted FLAIR is different from the commonly used susceptibility-weighted imaging at high field strength, as direct susceptibility effects are reversed in a spin echo. Indirectly, susceptibility effects may play a role as spin diffusion through susceptibility-induced field gradients may yield irreversible signal loss.

A limitation of the present study is that the current SAR limitations did not allow for full brain coverage at 7 T in a reasonable scan time. Reducing the number of slices resulted in a wider temporal spacing of the adiabatic inversion pulses (longer TR) and thus in a reduction in the SAR. Full brain coverage could be obtained at the cost of two extra interleaves, leading to a longer imaging time of approximately 10 min. Moreover, even more slices would be required if one would exploit the gain in SNR to obtain a higher resolution. Therefore, further developments are certainly required to obtain an adequate high resolution T_2-weighted FLAIR protocol at 7 T. A possible solution for full brain coverage within a reasonable imaging time is the implementation of B_1 shimming, which may allow a less

SAR demanding inversion pulse to be used. The use of low refocusing flip angles may also greatly reduce SAR, while T_2 contrast can be preserved by increasing the echo train length.

In the present study a slightly shorter echo time was used at 7 T to compensate for a shorter T_2 at this field strength. Owing to the somewhat higher (nominal) B_1 available at 7 T, the shorter echo time was possible without significant change in the receiver bandwidth, which makes the SNR directly comparable among the field strengths. However, the TR was longer at 7 T, which may have led to a difference in the amount of signal loss from magnetisation transfer. Furthermore there was a difference in the receive coils used, with a 16-channel receive coil used at 7T and 8-channel receive coils at 1.5 T and 3 T, which also may have contributed to the observed increase in SNR at 7 T. As the inhomogeneity in both transmit and receive fields requires new solutions with multiple coils at high field strength [19], one may regard the gain in SNR observed in the studied region as an indication of the potential of FLAIR at 7 T.

A limitation that FLAIR imaging has in common with other imaging techniques at 7 T is the sensitivity to variations in transmit field and a relative low RF power in the temporal lobes and the frontal and temporal operculum. Consequently, there is a major drop in signal in these regions. Future developments and optimisation of multichannel transmit options should provide a solution for a more homogeneous intensity throughout the brain.

In conclusion, we demonstrate the potential of T_2-weighted FLAIR imaging at 7 T with a high SNR and contrast that allow the depiction of anatomical detail such as white matter substructures in addition to the depiction of white matter lesions. Furthermore, the increase in contrast

of white matter substructures and deep brain structures show that FLAIR imaging at 7 T may be a valuable addition to MR neuroimaging protocols at this ultra-high field strength.

References

1. Hajnal JV, De CB, Lewis PD, Baudouin CJ, Cowan FM, Pennock JM, Young IR, Bydder GM (1992) High signal regions in normal white matter shown by heavily T2-weighted CSF nulled IR sequences. J Comput Assist Tomogr 16:506–513

2. Barkhof F, Scheltens P (2002) Imaging of white matter lesions. Cerebrovasc Dis 13(Suppl 2):21–30

3. Moraal B, Roosendaal SD, Pouwels PJ, Vrenken H, van Schijndel RA, Meier DS, Guttmann CR, Geurts JJ, Barkhof F (2008) Multi-contrast, isotropic, single-slab 3D MR imaging in multiple sclerosis. Eur Radiol 18:2311–2320

4. Chagla GH, Busse RF, Sydnor R, Rowley HA, Turski PA (2008) Three-dimensional fluid attenuated inversion recovery imaging with isotropic resolution and nonselective adiabatic inversion provides improved three-dimensional visualization and cerebrospinal fluid suppression compared to two-dimensional flair at 3 tesla. Invest Radiol 43:547–551

5. Tkac I, Gruetter R (2005) Methodology of H-1 NMR spectroscopy of the human brain at very high magnetic fields. Appl Magn Reson 29:139–157

6. Duyn JH, van GP, Li TQ, de Zwart JA, Koretsky AP, Fukunaga M (2007) High-field MRI of brain cortical substructure based on signal phase. Proc Natl Acad Sci U S A 104:11796–11801

7. Cho ZH, Kang CK, Han JY, Kim SH, Kim KN, Hong SM, Park CW, Kim YB (2008) Observation of the Lenticulostriate Arteries in the Human Brain In Vivo Using 7.0T MR Angiography. Stroke. doi:10.1161/STROKEAHA.107.508002

8. Hendrikse J, Zwanenburg JJ, Visser F, Takahara T, Luijten P (2008) Noninvasive depiction of the lenticulostriate arteries with time-of-flight MR angiography at 7.0 T. Cerebrovasc Dis 26:624–629

9. Gati JS, Menon RS, Ugurbil K, Rutt BK (1997) Experimental determination of the BOLD field strength dependence in vessels and tissue. Magn Reson Med 38:296–302

10. Yacoub E, Shmuel A, Pfeuffer J, van de Moortele PF, Adriany G, Andersen P, Vaughan JT, Merkle H, Ugurbil K, Hu X (2001) Imaging brain function in humans at 7 Tesla. Magn Reson Med 45:588–594

11. Tallantyre EC, Brookes MJ, Dixon JE, Morgan PS, Evangelou N, Morris PG (2008) Demonstrating the perivascular distribution of MS lesions in vivo with 7-Tesla MRI. Neurology 70:2076–2078

12. Garwood M, Delabarre L (2001) The return of the frequency sweep: designing adiabatic pulses for contemporary NMR. J Magn Reson 153:155–177

13. Rooney WD, Johnson G, Li X, Cohen ER, Kim SG, Ugurbil K, Springer CS Jr (2007) Magnetic field and tissue dependencies of human brain longitudinal $^{1}H_2O$ relaxation in vivo. Magn Reson Med 57:308–318

14. Phal PM, Usmanov A, Nesbit GM, Anderson JC, Spencer D, Wang P, Helwig JA, Roberts C, Hamilton BE (2008) Qualitative comparison of 3-T and 1.5-T MRI in the evaluation of epilepsy. AJR Am J Roentgenol 191:890–895

15. Runge VM, Case RS, Sonnier HL (2006) Advances in clinical 3-tesla neuroimaging. Invest Radiol 41:63–67

16. Schwindt W, Kugel H, Bachmann R, Kloska S, Allkemper T, Maintz D, Pfleiderer B, Tombach B, Heindel W (2003) Magnetic resonance imaging protocols for examination of the neurocranium at 3 T. Eur Radiol 13:2170–2179

17. Bachmann R, Reilmann R, Schwindt W, Kugel H, Heindel W, Kramer S (2006) FLAIR imaging for multiple sclerosis: a comparative MR study at 1.5 and 3.0 Tesla. Eur Radiol 16:915–921

18. Haacke EM, Xu Y, Cheng YC, Reichenbach JR (2004) Susceptibility weighted imaging (SWI). Magn Reson Med 52:612–618

19. Wiesinger F, van de Moortele PF, Adriany G, De Zanche N, Ugurbil K, Pruessmann KP (2006) Potential and feasibility of parallel MRI at high field. NMR Biomed 19:368–378